JOURNAL OF MATERIALS SCIENCE 23 (1988) 905–913

Microstructural observation and reaction mechanism of $ZnAl_2O_4$ formation in the presence of various fluorides

M. HASHIBA, Y. NURISHI, T. HIBINO
Department of Industrial Chemistry, Faculty of Engineering, Gifu University: Yanagido, Gifu-shi 501-11, Japan

The rates of $ZnAl_2O_4$ formation in the presence of various fluorides were controlled by the nucleation process. The rate constants of the nucleation process for various fluorides were in the order LiF > NaF and MgF_2 > CaF_2 < SrF_2 < BaF_2. This trend corresponds to the order of the promotion of $ZnAl_2O_4$ formation by these fluorides. In order to interpret the dependence of the kinetic constant of the nucleation of $ZnAl_2O_4$ from the intermediate phase on the kinds of counter cation of fluorides, it was assumed that the activated state for promotive formation of $ZnAl_2O_4$ under the presence of fluoride is similar to that of the following reaction:

$$ZnO + Al_2O_3 + 2MF(M'F_2) = ZnF_2 + M_2Al_2O_4(M'Al_2O_4).$$

The order of the rate constant obtained in this study showed agreement with the order of the standard heats of formation for the above reaction. This relation was interpreted by applying the linear free energy relationship (LFER).

1. Introduction

In a solid state reaction, successive investigations must be made on the reaction processing from starting materials to the extent of reaction. It is important to control processing which may affect the solid state reaction rates and to characterize materials and the process in order to obtain reliable and reproducible kinetic data for the reaction [1].

Many additives (intentionally added impurity) have been tested to determine whether they promote solid state reactions as sintering aids or promotive agents [2–11]. However, it has not been possible to elucidate the detailed role of impurities or additives in a solid state reaction.

In some cases, in spite of the addition of the same additives, different results were obtained by the various investigators. Thus, it is necessary to bear in mind that the different effects of additive must be attributed to the different physical properties of raw materials, the different mixing methods, the different forming method and the different firing conditions, etc.

It has been reported that $ZnAl_2O_4$ formation from alumina and zinc oxide with lithium fluoride is affected by the particle size of alumina [12], the physical nature of alumina (aggregates or agglomerates of alumina) and compaction pressures used when forming the specimen compacts [13]. In the reaction mixture including LiF, coarse Al_2O_3 and fine ZnO particles [14], an intermediate liquid phase which contained LiF, Al_2O_3 and ZnO was found around the alumina particles by the microstructural observation. The formation of $ZnAl_2O_4$ was promoted by the rapid migration of raw materials through this intermediate phase. Thus, it turned out that the observation of microstructure is really a key to examine $ZnAl_2O_4$ formation with fluoride, because the microstructure is the result of the behaviour of the reactants, products and additives.

The purpose of the present work was the investigation of the effect of various fluorides such as LiF, NaF and alkaline earth fluorides on $ZnAl_2O_4$ formation by observing the microstructural changes during the reaction under various conditions. The microstructure of $ZnAl_2O_4$ formed from ZnO and an agglomerate of fine Al_2O_3 particles which had been prepared by spray drying was compared with that from coarse Al_2O_3 and ZnO particles.

2. Experimental procedure

2.1. Materials

Alpha-alumina, primary particle size 0.2 μm, Aluminum Co., America (Alcoa A-16 SG), was used as the starting material. By spray-drying the α-alumina, agglomerated alumina of 40 μm average size was prepared. The source of ZnO was GR grade of 0.3 μm average size, Kishida Chemicals Co. Fluorides were extra-pure reagent from Nakarai Chemicals Co.

2.2. Sample preparation and firing

20 mol % of each fluoride was added to an equivalent molar mixture of ZnO and agglomerated Al_2O_3. The compacts were heated in an electric furnace at a temperature between 600 and 1000° C for various durations in an argon atmosphere.

0022–2461/88 $03.00 + .12

2.3. Phase analysis and microstructural observation

Phases in the fired specimens were identified using conventional powder technique by X-ray (XRD) analysis (Jeol Model JDX 7E). Green and fired compacts were impregnated in epoxy resin and ground and finally polished with 2 μm diamond paste. Polished samples were observed by optical microscopy in reflected light and also by a scanning electron microscopy (SEM). The chemical composition of the phase in the microstructure was analysed by energy dispersive X-ray microanalyser (EDX) (Horiba Ltd, model EMAX 8000 S) attached to the SEM. An Hitachi Model H 800 transmission electron microscope was also employed to determine the particle size of the starting powders.

2.4. Determination of the extent of $ZnAl_2O_4$ formation

The extent of $ZnAl_2O_4$ formation was calculated from the amount of residual ZnO. The latter was determined chemically by dissolving ZnO with 2 mol dm^{-3} HCl solution and titrating Zn^{2+} with 0.01 mol dm^{-3} EDTA solution with EBT as the indicator at pH 10. XRD analysis was applied for the determination of the extent of $ZnAl_2O_4$ formation in the presence of alkaline earth fluorides.

3. Results and discussion

3.1. The rate of formation of $ZnAl_2O_4$ from ZnO and agglomerates of fine Al_2O_3 in the presence of various fluorides

Fig. 1 shows the formation rate of $ZnAl_2O_4$ from ZnO and agglomerates of fine Al_2O_3 in the presence of LiF. The formation of $ZnAl_2O_4$ seems to begin appreciably at about 600° C. The amount of $ZnAl_2O_4$ rapidly increased up to a certain limit (α_{max}) of almost constant value in an early stage of reaction. Sometimes sigmoidal curves were obtained at a low firing temperature.

In the case of other fluorides, i.e. NaF, MgF_2, CaF_2, SrF_2 and BaF_2, $ZnAl_2O_4$ formation began at about 700° C and the rate followed similar sigmoidal curves with different limits. The amounts of $ZnAl_2O_4$ present at the limit were plotted for each fluoride in Fig. 2: the amounts at the limit were in the following order, LiF > NaF, MgF_2 > CaF_2 < SrF_2 < BaF_2 at 700° C. Similar results were obtained for the effect of fluorides on $MgAl_2O_4$ formation [15].

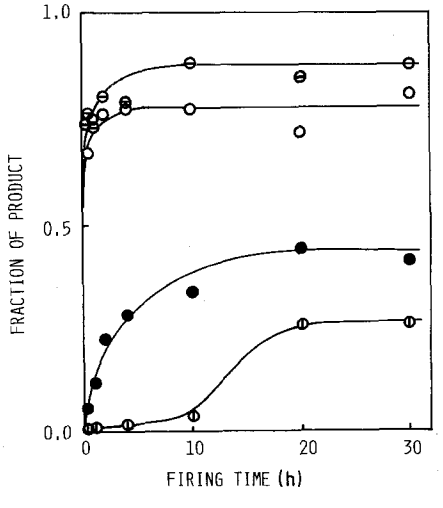

Figure 1 Rate curves of $ZnAl_2O_4$ formation in the presence of LiF at (Φ) 600° C, (●) 700° C, (○) 800° C, (⊖) 900° C.

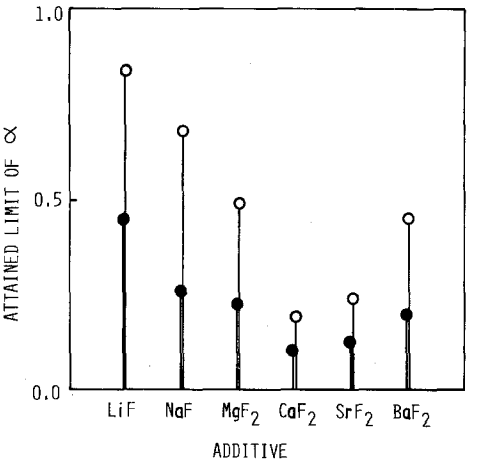

Figure 2 Attained limit values of extent of $ZnAl_2O_4$ formation plotted for each fluoride at (●) 700° C and (○) 800° C.

The rate curves were analysed by Hancock and Sharp's method [16]. The values of ln ln [1/(1 − α)] were calculated from the extent of $ZnAl_2O_4$ formation, α, and plotted against the logarithm of the firing time, ln t (Fig. 3).

The process with a slope of 2 corresponds to a nucleation controlled reaction. The nucleation process was followed by a process with a low slope of 0.5 which corresponds to a diffusion controlled reaction [17]. For LiF, which gave a sigmoidal curve, a step with low slope of 0.5, which would be a diffusion process, preceded the nucleation process. Transport of

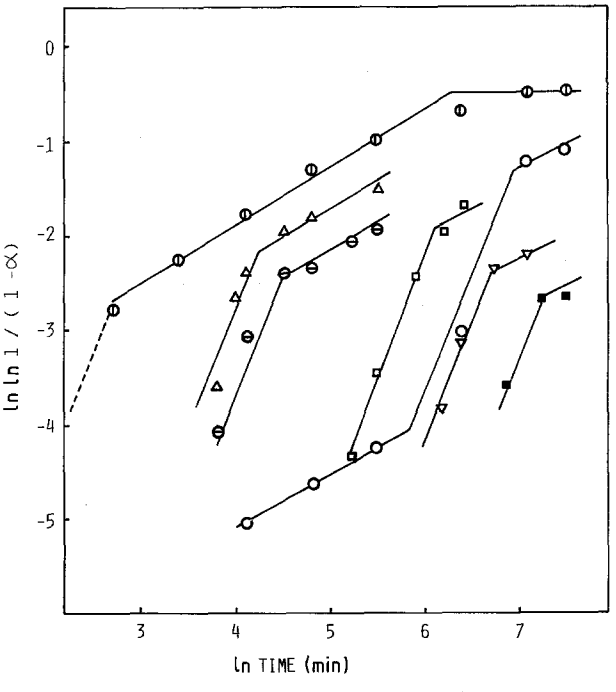

Figure 3 Analysis of the rate curves obtained at a low temperature for $ZnAl_2O_4$ formation with each fluoride using Hancock and Sharp's method. (Φ) LiF, 700° C, (△) NaF, 700° C, (⊖) MgF_2, 700° C, (□) BaF_2, 700° C, (○) LiF, 600° C, (▽) SrF_2, 700° C (■) CaF_2, 700° C.

0022–2461/88 $03.00 + .12

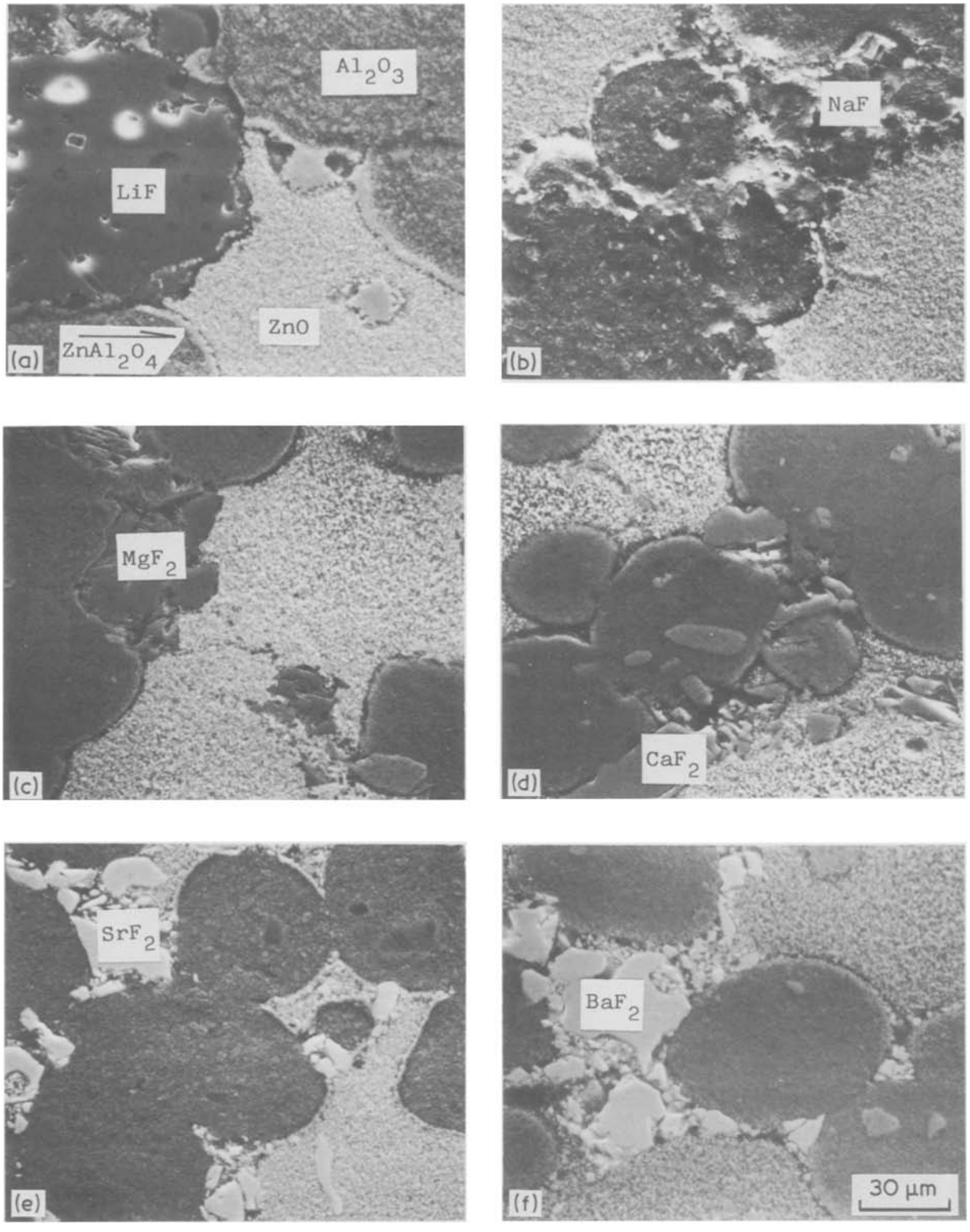

Figure 4 Microstructures in the formation of $ZnAl_2O_4$ in the presence of various fluoride salts; specimens were fired at 700° C for 10 h. (a) LiF, (b) NaF, (c) MgF_2, (d) CaF_2, (e) SrF_2, (f) BaF_2.

fluoride liquid or dissolution of oxides in fluoride liquid could possibly be the preceded step.

Apparent rate constants for the nucleation controlled process are shown in Table I and are in the order LiF > NaF, and $MgF_2 > CaF_2 < SrF_2 < BaF_2$, similar to the order for α_{max}. Lithium fluoride and sodium fluoride gave larger promotive effects for $ZnAl_2O_4$ formation rate than that of alkaline earth fluorides. Among the alkaline earth fluorides, calcium fluoride showed the minimum promotion and barium fluoride was most promotive.

3.2. Microstructural changes at 700° C

At 700° C, which is close to the starting temperature of $ZnAl_2O_4$ formation, a thin $ZnAl_2O_4$ layer with many interspaces was produced at the alumina side of the boundary zone between zinc oxide and alumina for all fluoride additives, as indicated in Fig. 4. In the process zinc oxide was mainly transported by diffusion through the fluoride liquid into the Al_2O_3 phase. However, after a long firing time, small $ZnAl_2O_4$ particles were found in the ZnO phase. This fact indicates that the transport of Al_2O_3 to the ZnO

TABLE I Apparent rate constants of nucleation-controlled reaction of $ZnAl_2O_4$ formation in the presence of fluoride additives

Fluoride	ln k (min^{-1})	
	700° C	600° C
LiF	−10.7	−21.8
NaF	−14.6	
MgF_2	−15.6	
CaF_2	−24.4	
SrF_2	−22.2	
BaF_2	−20.0	

phase occurred at the same time, although its rate was very small.

After long firing times, a diffuse layer of zinc was observed in the alumina agglomerate. Lithium aluminate, $LiAl_5O_8$, for LiF addition, β-alumina for NaF addition, and $MgAl_2O_4$ for MgF_2 addition, were confirmed in the diffuse layer of zinc in the Al_2O_3 phase. These results show that the intermediate phase penetrated into the agglomerates of Al_2O_3 with dissolution of Al_2O_3. Fig. 5 shows a schematic reaction model for the specimen with the agglomerates of alumina in the presence of LiF.

3.3. Discussion of the mechanism of $ZnAl_2O_4$ formation in the presence of various fluorides

Here the dependence of the kinetic constant of the nucleation of $ZnAl_2O_4$ on the kind of fluoride cation is discussed. There are no available thermodynamic and kinetic data based on the interaction for the fluoride–oxide liquid mixtures.

It is well known that a group of reactions can be interpreted by the linear free energy relationship (LFER) [18], i.e. a linear relationship between logarithm of the rate constants and logarithm of equilibrium constants and its possible extension to a linear relationship between the activated enthalpy and the heat of reaction. For example, Seiyama [19] has described that in the oxidation of ethylene a linear relationship is set up between the extent of reaction and the heat of formation of metal oxide used as a catalyst. He has explained that the strength of the metal–oxygen bond affects the rate-determining step of the reaction.

In this study the idea of LFER was also applied for the analysis of $ZnAl_2O_4$ formation. The rate constants of $ZnAl_2O_4$ formation for the nucleation process obtained from Hancock and Sharp's analysis was compared with the enthalpy changes of Reaction 1, which is assumed to be equilibrated with the activated state of the nucleation process. Reaction 1 may be evaluated by the enthalpy changes instead of the free energy changes of reaction because the entropy changes of the reaction show only small differences among the kinds of fluorides.

$$ZnO + Al_2O_3 + 2MF(M'F_2) = ZnF_2 + M_2Al_2O_4(M'Al_2O_4) \quad (1)$$

The enthalpy changes of Reaction 1 [20–25] are shown in Table II. As seen in Table II, the enthalpy

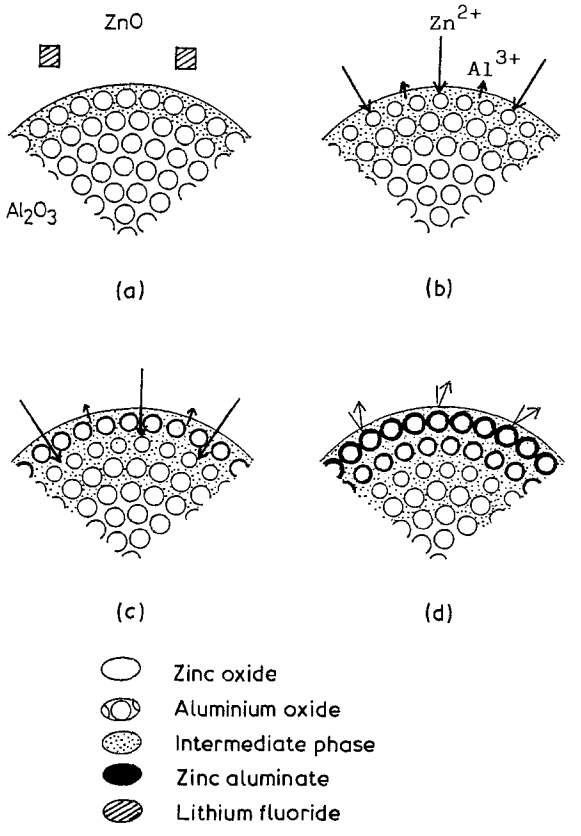

Figure 5 Schematic reaction model for the specimen with agglomerated Al_2O_3 in the presence of LiF.

changes of the aluminate formation were estimated from the heat of formation from their constituent oxides. Fig. 6 shows the interrelationship between the rate constants and the enthalpy changes of Reaction 1. Good correlation is found between the rate constants and the enthalpy changes of Reaction 1. It was reported in the previous section that the order of the rate constants is similar to the order of α_{max}. Fig. 7 shows the relationship between α_{max} and the enthalpy

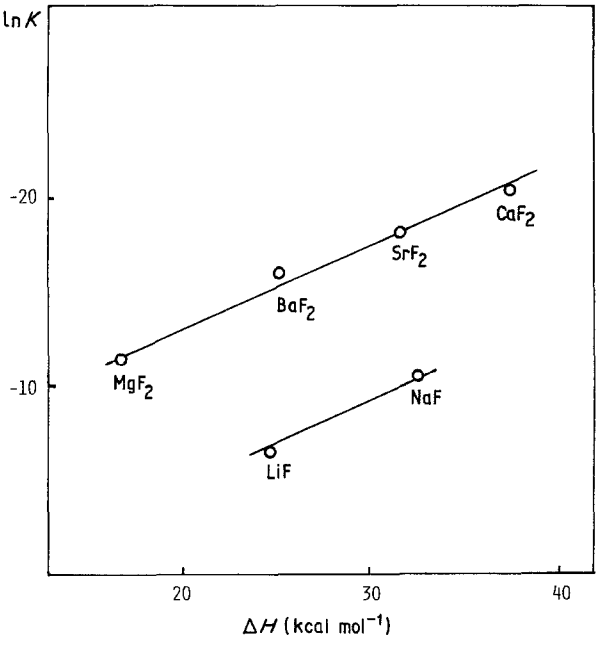

Figure 6 Correlation between rate constants and the enthalpy changes of Reaction 1.

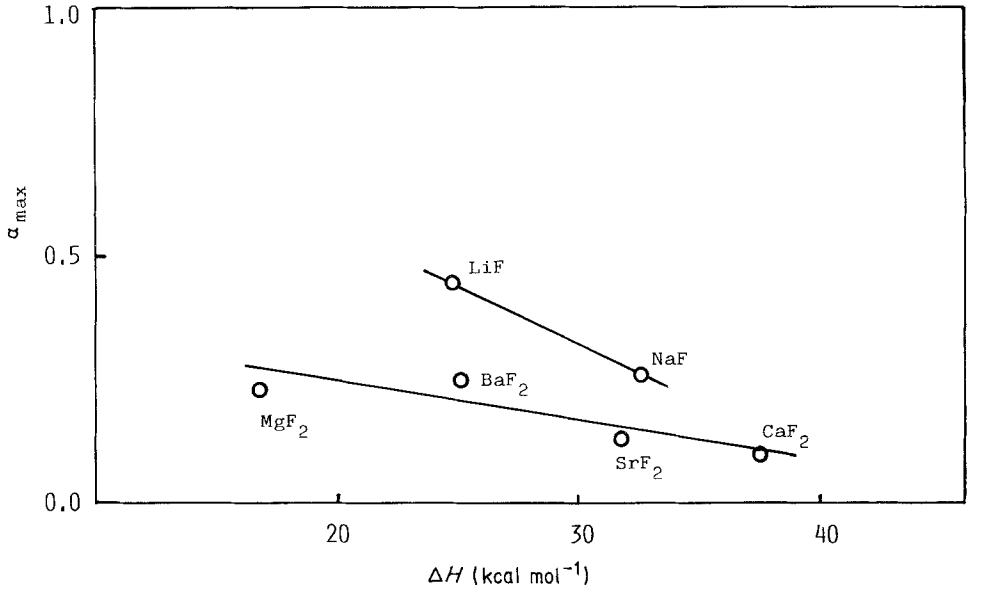

Figure 7 Relationship between maximum value of the extent of reaction and the enthalpy changes of Reaction 1.

changes of Reaction 1. This result seems to suggest that the reaction having a large rate constant would increase the yield. The formation of $ZnAl_2O_4$ in the presence of fluoride appears to proceed in such a scheme as shown in Fig. 8. The results obtained in this study support the results of the previous paper, i.e. we [15] have estimated that the activated state for promotive formation of $MgAl_2O_4$ is similar to that of the following reaction where three components of reactants and the additive fluoride interact simultaneously.

$$MgO + Al_2O_3 + 2MF(M'F_2) = MgF_2 + M_2Al_2O_4(M'Al_2O_4) \quad (2)$$

Good correlation was found between the enthalpy changes of Reaction 2 and the amount of $MgAl_2O_4$. For example, in the case of addition of alkaline earth fluorides, the amount of $MgAl_2O_4$ was in the order $MgF_2 > CaF_2 < SrF_2 < BaF_2$. The enthalpy changes of Reaction 2 indicated the order $MgF_2 < CaF_2 > SrF_2 > BaF_2$. The small value of enthalpy changes of Reaction 2 corresponded to a large amount of $MgAl_2O_4$ being promoted by a fluoride, compared with others.

Shimada *et al.* [26, 27] have already indicated that in the reaction between MgO an Al_2O_3 with fluoride, AlF_3 formed prior to the formation of $MgAl_2O_4$ and the formation of AlF_3 was promoted by MgO. They evaluated the promotion of $MgAl_2O_4$ formation by the enthalpy change of the following reaction:

$$4Al_2O_3 + 6MF = 2AlF_3 + 3M_2Al_2O_4$$
$$4Al_2O_3 + 3M'F_2 = 2AlF_3 + 3M'Al_2O_4 \quad (3)$$

The present analysis is essentially compatible with that by Shimada *et al.*

3.4. Microstructural changes above 800° C

At 800° C, for LiF addition, $ZnAl_2O_4$ was mainly observed in the ZnO phase in contrast to the case at 700° C. Many coarse $ZnAl_2O_4$ crystals were formed in the ZnO phase by transport of Al_2O_3 through the

TABLE II The enthalpy changes (kcal mol^{-1} at 298 K) of Reaction 1 for various metal fluorides

Fluorides	ΔH^0 (MA)*	ΔH^0 (MO)	ΔH^0 (ZnF_2)	$-\Delta H^0$ (2MF) ($M'F_2$)	$-\Delta H^0$ (ZnO)	ΔH (Eq. 1)
LiF	−25.7	−142.6	−182.7	292.6	83.2	24.8
NaF	−41.8	−100.7	−182.7	274.6	83.2	32.6
KF		−86.4	−182.7	269.0	83.2	
RbF		−68.0	−182.7	262.6	83.2	
CsF		−75.9	−182.7	253.8	83.2	
BeF_2	−4.0	−143.1	−182.7	243.0	83.2	−3.6
MgF_2	−6.0	−143.7	−182.7	266.0	83.2	16.8
CaF_2	−3.7	−151.6	−182.7	292.0	83.2	37.2
SrF_2	−13.8	−144.2	−182.7	289.0	83.2	31.5
BaF_2	−24.0	−139.0	−182.7	287.7	83.2	25.2
MnF_2	−10.0	−92.0	−182.7	190.0	83.2	−11.5
FeF_2	−10.7	−63.2	−182.7	168.0	83.2	−5.4
CoF_2	−9.0	−57.1	−182.7	159.0	83.2	−6.6
NiF_2	−0.7	−57.5	−182.7	158.0	83.2	0.3
CuF_2	5.0	−37.1	−182.7	128.0	83.2	−3.6
ZnF_2	−10.5	−83.2	−182.7	182.7	83.2	−10.5
CdF_2	4.5	−61.1	−182.7	167.4	83.2	11.3

*From oxides.

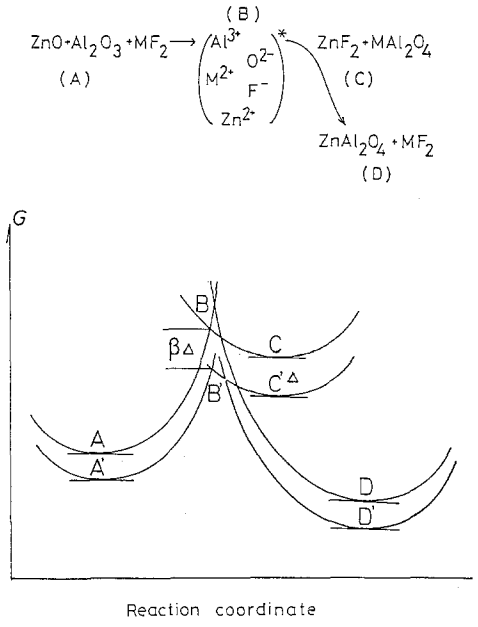

Figure 8 Schematic free energy diagram for the formation of $ZnAl_2O_4$ in the presence of fluoride.

interspace of the $ZnAl_2O_4$ layer without forming aluminate with additive fluoride (Fig. 9a). The maps of zinc and aluminium distribution at 800° C by EDX analysis were shown in Fig. 9b and c. They suggest that aluminium was carried by the fluoride liquid from the Al_2O_3 phase to the ZnO phase, whereas a small amount of zinc moved from the ZnO phase to the Al_2O_3 phase.

When agglomerated Al_2O_3 was used as a starting material, a $ZnAl_2O_4$ layer having many interspaces was produced. Through the interspaces fluoride liquid carries Al_2O_3 to the ZnO phase and $ZnAl_2O_4$ forms in the ZnO phase without $LiAl_5O_8$. On the other hand, on addition of NaF, formation of $ZnAl_2O_4$ was found in the agglomerated Al_2O_3 in addition to the formation of β-Al_2O_3.

As previously reported [14], dense and coarse Al_2O_3 as a starting material formed a dense $ZnAl_3O_4$ layer around the Al_2O_3. This layer confines a liquid phase between the Al_2O_3 and the dense $ZnAl_2O_4$ layer and interrupts the spread of the liquid to the ZnO phase. $ZnAl_2O_4$ formation in the ZnO phase was, therefore, largely suppressed because of slow diffusion of Zn^{2+} through the dense $ZnAl_2O_4$ layer. Moreover, $LiAl_5O_8$, deposited on the spinel–liquid interface and interrupted the material transport, as indicated in Fig. 10.

At 900° C, $ZnAl_2O_4$ was mainly formed in the ZnO phase when LiF or NaF was added, whereas $ZnAl_2O_4$ grew into agglomerates of Al_2O_3 phase in the case of alkaline earth fluoride.

At 1000° C, in the case of MgF_2 or CaF_2 addition, zinc aluminate formed mainly within the Al_2O_3 agglomerate phase at all firing temperatures examined. However, the function of additive was different between MgF_2 and CaF_2. For MgF_2 addition, the magnesium ions competed with the zinc ions to react with alumina in the Al_2O_3 agglomerate phase to form each spinel, and $MgAl_2O_4$ co-existed with $ZnAl_2O_4$ in Al_2O_3 agglomerate phase as shown in Fig. 11. In this case the fluoride ion must, therefore, work as aluminium fluoride or oxyfluoride by reaction with Al_2O_3. On CaF_2 addition, the calcium ion was found as calcium fluoride in the X-ray diffraction patterns and also in the microstructure shown in Fig. 12. Formation of $ZnAl_2O_4$ even in the ZnO phase was observed for the case of SrF_2 and BaF_2 addition as shown in Fig. 13. The conditions determining whether $ZnAl_2O_4$ mainly

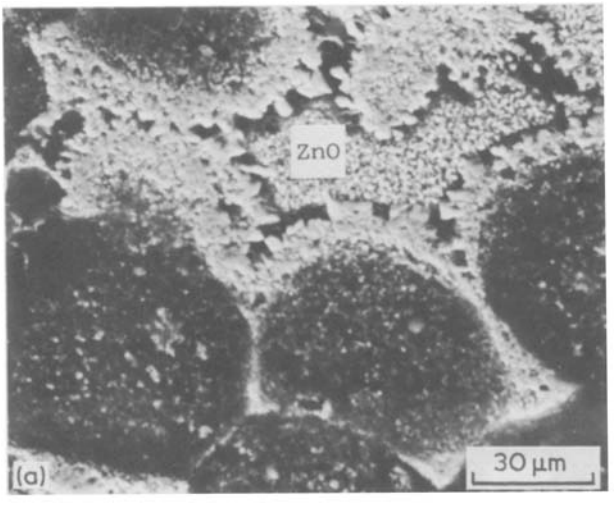

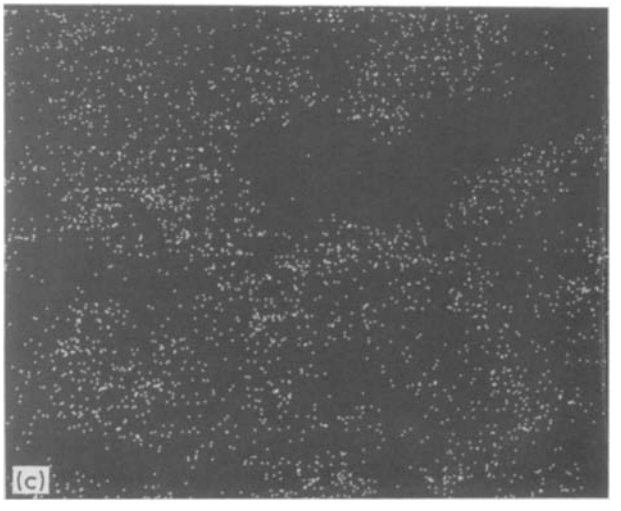

Figure 9 SEM and EDX analyses of $ZnAl_2O_4$ formation in a specimen of agglomerate of fine Al_2O_3, ZnO and LiF fired at 800° C for 20 h. (a) SE image, (b) X-ray image of zinc, (c) X-ray image of aluminium.

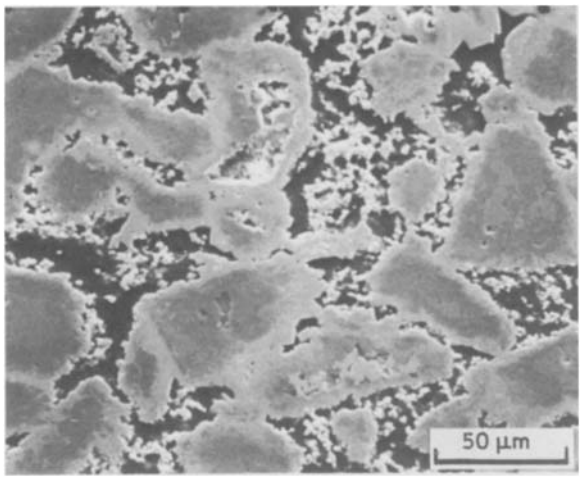

Figure 10 Microstructure of $ZnAl_2O_4$ formation in a specimen of coarse Al_2O_3, ZnO and LiF fired at 800° C for 20 h.

forms in Al_2O_3 phase or ZnO phase depend on the starting form of Al_2O_3, on the firing temperature and on the kind of fluoride cation.

It is interesting to consider the formation conditions of aluminates other than $ZnAl_2O_4$. The liquid fluoride phase dissolves ZnO, Al_2O_3 and contains the cations of the fluoride additive. Its composition depends on the physical and chemical properties of $ZnAl_2O_4$ and of alumina and ZnO. If the liquid can easily spread and soaks into ZnO powder, $ZnAl_2O_4$ formation is maximized. If a dense $ZnAl_2O_4$ wall is formed first, the

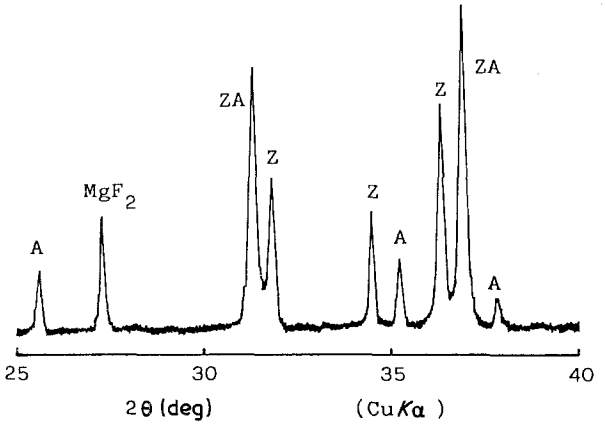

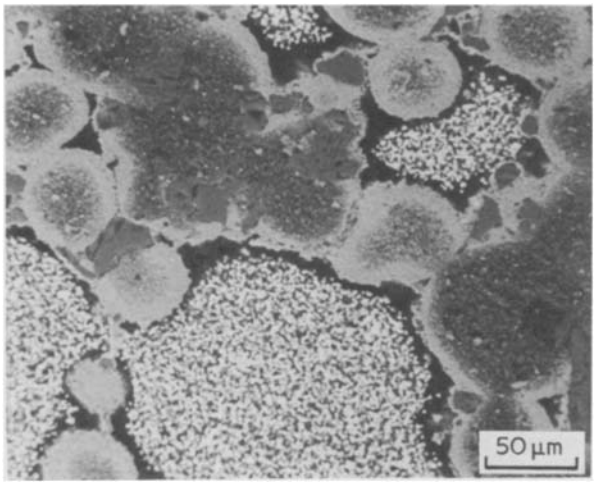

Figure 11 XRD pattern and microstructure for the specimen with MgF_2 fired at 1000° C for 1 h.

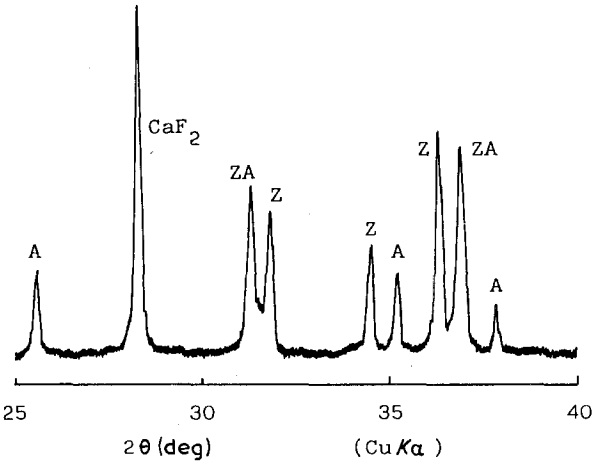

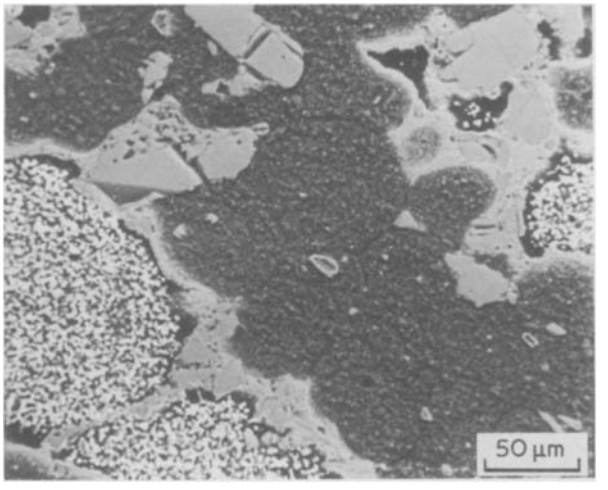

Figure 12 XRD pattern and microstructure for the specimen with CaF_2 fired at 1000° C for 1 h.

permeation of Zn^{2+} into the liquid is prevented and no more $ZnAl_2O_4$ is formed; the other aluminate becomes saturated instead. The solubility of oxides in the melt and the viscosity, wettability, and melting point of the molten fluoride depend on its cationic species. The agglomerated state of starting oxide materials seems to lead to further complications.

3.5. Controlling factor of main position of $ZnAl_2O_4$ formation in each microstructure

Fig. 14 shows the site in the oxide mixture where $ZnAl_2O_4$ formation proceeds, in relation to temperature as the ordinate and the kind of fluorides as the abscissa.

At a low firing temperature close to the starting temperature, $ZnAl_2O_4$ is formed mainly in the alumina phase. This indicates that transport of Al_2O_3 through the intermediate liquid could not be expected at this stage because dissolution of alumina would be difficult. From the rate analysis at the starting temperature of $ZnAl_2O_4$ formation it was expected that on addition of LiF, the slow diffusion process preceded the nucleation process. Thus, zinc oxide was transported through the intermediate phase on to alumina surface and nucleated as $ZnAl_2O_4$ on Al_2O_3 phase. Its process sometimes accompanies the formation of aluminate of the additive cation.

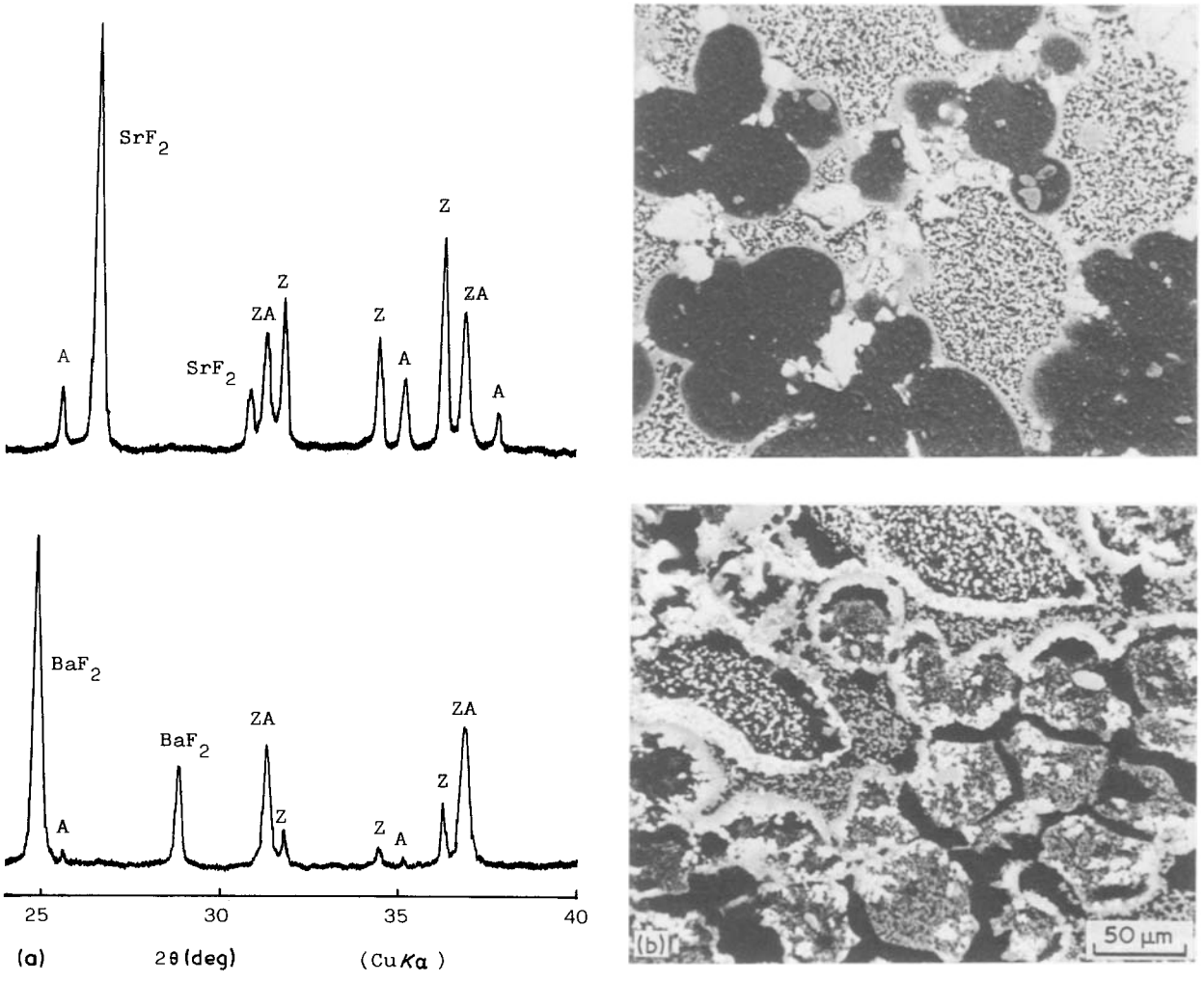

Figure 13 (a) X-ray diffraction patterns in the specimens with SrF_2 and BaF_2; the specimens were fired at 1000° C for 1 h. The upper half and lower half in XRD patterns indicate the results for the specimens containing SrF_2 and BaF_2, respectively. (b) Microstructures of the specimens with SrF_2 or BaF_2; the specimens were fired at 1000° C for 1 h. The upper half and the lower half of the micrographs indicate the results for the specimens containing SrF_2 and BaF_2, respectively.

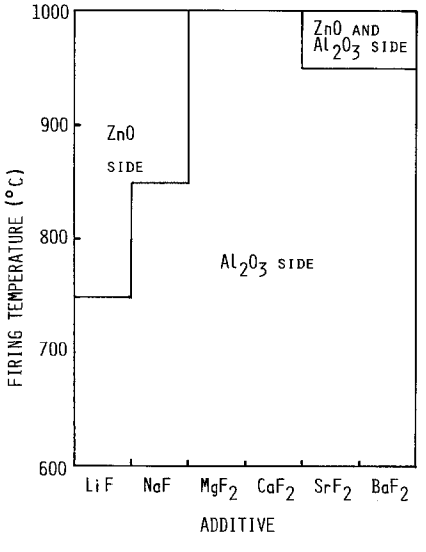

Figure 14 Location of $ZnAl_2O_4$ which was mainly formed in the presence of fluoride salts. ZnO side: $ZnAl_2O_4$ has developed into agglomerates of fine ZnO phase. Al_2O_3 side: $ZnAl_2O_4$ has developed into agglomerates of fine Al_2O_3 phase. ZnO and Al_2O_3 sides: $ZnAl_2O_4$ has formed at the interface between Al_2O_3 and ZnO agglomerates.

With increasing firing temperature, $ZnAl_2O_4$ starts to develop in the ZnO phase. Transport of alumina by way of the fluoride liquid through interspaces of the $ZnAl_2O_4$ layer become apparent without intervention due to the formation of aluminates of the additive cations.

A change in main position of $ZnAl_2O_4$ formation from Al_2O_3 phase to ZnO phase implies that the transport of the alumina to the ZnO phase through the intermediate phase becomes possible due to the rapid dissolution of alumina by the intermediate phase.

4. Conclusions

The effects of various fluorides on the $ZnAl_2O_4$ formation were examined and discussed. The rates of $ZnAl_2O_4$ formation in the presence of various fluorides were controlled by the nucleation process. The rate constants of the nucleation process for various fluorides were in the order LiF > NaF and $MgF_2 > CaF_2 < SrF_2 < BaF_2$. This trend corresponds to the order of the promotion of $ZnAl_2O_4$ formation by these fluorides. In order to interpret the

dependence of the kinetic constant of the nucleation of $ZnAl_2O_4$ from the intermediate phase on the kinds of counter cation of fluoride, it was assumed that the activated state for promotive formation of $ZnAl_2O_4$ in the presence of fluoride is similar to that of Reaction 1. The order of the rate constant obtained in this study showed agreement with the order of the standard heats of formation for Reaction 1. This relation was interpreted by applying the linear free energy relationship (LFER).

The main formation site of $ZnAl_2O_4$ from Al_2O_3 to the ZnO phase was changed by increasing the firing temperature and the kinds of fluorides. Alteration of this site of formation implies that the transport of alumina to the ZnO phase through the intermediate phase become possible due to the rapid dissolution of alumina by the intermediate phase.

References

1. H. OKADA, H. KAWAKAMI, M. HASHIBA, E. MIURA, Y. NURISHI and T. HIBINO, *J. Amer. Ceram. Soc.* **68** (1985) 58.
2. J. M. HAUSSONNE, G. DESGARDIN, Ph. BAJOLET and B. RAVEAU, *ibid.* **66** (1983) 801.
3. D. W. JOHNSON Jr, P. K. GALLAGHER and E. M. VOGEL, *Bull. Amer. Ceram. Soc.* **57** (1978) 751.
4. J. LEMAITRE and B. DELMON, *ibid.* **59** (1980) 234.
5. D. E. WITTMER and R. C. BUCHANAN, *J. Amer. Ceram. Soc.* **64** (1981) 485.
6. P. C. DOKKO and P. A. PASK, *ibid.* **62** (1979) 433.
7. K. YOSHIDA, M. HASHIBA, Y. NURISHI and T. HIBINO, *Yogyo-Kyokai-Shi* **84** (1976) 89.
8. E. MIURA, R. FURUMI, M. HASHIBA, Y. NBURISHI and T. HIBINO, *ibid.* **88** (1980) 577.
9. R. A. EPPLER, *J. Amer. Ceram. Soc.* **62** (1979) 47.
10. S. SHIMADA, R. FURUICHI and T. ISHII, *Bull. Chem. Soc. Jpn* **49** (1976) 1289.
11. T. TSUCHIDA, R. FURUICHI and T. ISHII, *Chem. Lett.* (1975) 1191.
12. M. HASHIBA, Y. NURISHI and T. HIBINO, *J. Mater. Sci.* (submitted).
13. *Idem, ibid.* (submitted).
14. M. HASHIBA, E. MIURA, Y. NURISHI and T. HIBINO, *Nippon Kagaku Kaishi* (1983) 501.
15. M. MIYAMOTO, M. HASHIBA, Y. NURISHI and T. HIBINO, *Yogyo Kyokai-Shi* **83** (1975) 341.
16. J. D. HANCOCK and J. H. SHARP, *J. Amer. Ceram. Soc.* **55** (1972) 74.
17. S. F. HULBERT, *J. Br. Ceram. Soc.* **6** (1969) 11.
18. J. O. EDWARDS, "Inorganic Reaction Mechanism" (Interscience, New York, 1970) p. 252.
19. T. SEIYAMA, "Kinzoku Sankabutsu to Fukugo Sankabutsu" (Kodansya, Tokyo, 1980) p. 375.
20. O. KUBASCHEWSKI, E. LL. EVANS and C. B. ALCOCK, "Metallurgical Thermochemistry" (Pergamon, Oxford, 1967) p. 304.
21. JANAF Thermochemical Tables, 2nd Edn (Dow Chemicals Co., Midland, Michigan, 1970 and 1974, 1975 Supplements).
22. I. BARIN and O. KNACKE, "Thermochemical Properties of Inorganic Substances" (Springer-Verlag, Berlin, 1973).
23. F. MULLER and O. J. KLEPPA, *J. Inorg. Nucl. Chem.* **35** (1973) 2673.
24. J. A. SHEARER and O. J. KLEPPA, *ibid.* **35** (1973) 1073.
25. J. D. TRETYAKOW and SCHMALZRIED, *Ber. Bunsen.* **69** (1965) 396.
26. S. SHIMADA, R. FURUICHI and T. ISHII, *Bull. Chem. Soc. Jpn* **47** (1974) 2026.
27. *Idem, ibid.* **47** (1974) 2031.

Received 1 April
and accepted 16 June 1987